Sussex Research Online

Two-photon fluorescence imaging with 30 fs laser system tunable around 1 micron

Article (Published Version)

Resan, Bojan, Aviles-Espinosa, Rodrigo, Kurmulis, Sarah, Licea-Rodriguez, Jacob, Brunner, Felix, Rohrbacher, Andreas, Artigas, David, Loza-Alvarez, Pablo and Weingarten, Kurt J (2014) Two-photon fluorescence imaging with 30 fs laser system tunable around 1 micron. Optics Express, 22 (13). pp. 16456-16461. ISSN 1094-4087

This version is available from Sussex Research Online: http://sro.sussex.ac.uk/id/eprint/72329/

This document is made available in accordance with publisher policies and may differ from the published version or from the version of record. If you wish to cite this item you are advised to consult the publisher's version. Please see the URL above for details on accessing the published version.

Copyright and reuse:
Sussex Research Online is a digital repository of the research output of the University.

Copyright and all moral rights to the version of the paper presented here belong to the individual author(s) and/or other copyright owners. To the extent reasonable and practicable, the material made available in SRO has been checked for eligibility before being made available.

Copies of full text items generally can be reproduced, displayed or performed and given to third parties in any format or medium for personal research or study, educational, or not-for-profit purposes without prior permission or charge, provided that the authors, title and full bibliographic details are credited, a hyperlink and/or URL is given for the original metadata page and the content is not changed in any way.

http://sro.sussex.ac.uk

Two-photon fluorescence imaging with 30 fs laser system tunable around 1 micron

Bojan Resan,[1,*] Rodrigo Aviles-Espinosa,[2] Sarah Kurmulis,[1] Jacob Licea-Rodriguez,[3] Felix Brunner,[1] Andreas Rohrbacher,[1] David Artigas,[2] Pablo Loza-Alvarez,[2] and Kurt J. Weingarten[1]

[1]*Time-Bandwidth Products AG, Ruetistrasse 12, 8952 Schlieren, Switzerland*
[2]*Institute of Photonic Sciences, Av. Carl Friedrich Gauss 3, 08860 Castelldefels, Spain*
[3]*Department of Optics, CICESE, 22860 Ensenada B.C., Mexico*
[*]*bojan.resan@jdsu.com*

Abstract: We developed a low-cost, low-noise, tunable, high-peak-power, ultrafast laser system based on a SESAM-modelocked, solid-state Yb tungstate laser plus spectral broadening via a microstructured fiber followed by pulse compression. The spectral selection, tuning, and pulse compression are performed with a simple prism compressor. The output pulses are tunable from 800 to 1250 nm, with the pulse duration down to 25 fs, and average output power up to 150 mW, at 80 MHz pulse repetition rate. We introduce the figure of merit (FOM) for the two-photon and multi-photon imaging (or other nonlinear processes), which is a useful guideline in discussions and for designing the lasers for an improved microscopy signal. Using a 40 MHz pulse repetition rate laser system, with twice lower FOM, we obtained high signal-to-noise ratio two-photon fluorescence images with or without averaging, of mouse intestine section and zebra fish embryo. The obtained images demonstrate that the developed system is capable of nonlinear (TPE, SHG) imaging in a multimodal operation. The system could be potentially used in a variety of other techniques including, THG, CARS and applications such as nanosurgery.

©2014 Optical Society of America

OCIS codes: (320.7160) Ultrafast technology; (320.7090) Ultrafast lasers; (180.4315) Nonlinear microscopy.

References and links

1. W. Denk, J. H. Strickler, and W. W. Webb, "Two-photon laser scanning fluorescence microscopy," Science **248**(4951), 73–76 (1990).
2. U. K. Tirlapur and K. König, "Targeted transfection by femtosecond laser," Nature **418**(6895), 290–291 (2002).
3. F. Bourgeois and A. Ben-Yakar, "Femtosecond laser nanoaxotomy properties and their effect on axonal recovery in C. elegans," Opt. Express **15**(14), 8521–8531 (2007).
4. G. J. Tserevelakis, S. Psycharakis, B. Resan, F. Brunner, E. Gavgiotaki, K. J. Weingarten, and G. Filippidis, "Femtosecond laser nanosurgery of sub-cellular structures in HeLa cells by employing Third Harmonic Generation imaging modality as diagnostic tool," J. Biophotonics **5**(2), 200–207 (2012).
5. S. I. C. O. Santos, M. Mathew, O. E. Olarte, S. Psilodimitrakopoulos, and P. Loza-Alvarez, "Femtosecond laser axotomy in Caenorhabditis elegans and collateral damage assessment using a combination of linear and nonlinear imaging techniques," PLoS ONE **8**(3), e58600 (2013).
6. M. Farsari and B. N. Chichkov, "Materials processing: two-photon fabrication," Nat. Photonics **3**(8), 450–452 (2009).
7. E.g. Chameleon laser from Coherent Inc. *http://www.coherent.com/products/?1557/Chameleon-Family* or Mai Tai laser from Newport *http://www.newport.com/Mai-Tai-One-Box-Tunable-Ultrafast-Lasers/368124/1033/info.aspx*
8. F. Brunner, G. J. Spühler, J. A. Au, L. Krainer, F. Morier-Genoud, R. Paschotta, N. Lichtenstein, S. Weiss, C. Harder, A. A. Lagatsky, A. Abdolvand, N. V. Kuleshov, and U. Keller, "Diode-pumped femtosecond Yb:KGd(WO4)2 laser with 1.1-W average power," Opt. Lett. **25**(15), 1119–1121 (2000).
9. F. Druon, F. Balembois, and P. Georges, "New materials for short-pulse amplifiers," IEEE Photon. J. **3**(2), 268–273 (2011).
10. S. Ricaud, A. Jaffres, K. Wentsch, A. Suganuma, B. Viana, P. Loiseau, B. Weichelt, M. Abdou-Ahmed, A. Voss, T. Graf, D. Rytz, C. Hönninger, E. Mottay, P. Georges, and F. Druon, "Femtosecond Yb:CaGdAlO4 thin-disk oscillator," Opt. Lett. **37**(19), 3984–3986 (2012).

#212997 - $15.00 USD Received 28 May 2014; revised 18 Jun 2014; accepted 19 Jun 2014; published 26 Jun 2014

11. P. S. J. Russell, "Photonic crystal fibers," Science **299**(5605), 358–362 (2003).
12. J. M. Dudley, G. Genty, and S. Coen, "Supercontinuum generation in photonic crystal fiber," Rev. Mod. Phys. **78**(4), 1135–1184 (2006).
13. www.nkt.com
14. D. Kobat, M. E. Durst, N. Nishimura, A. W. Wong, C. B. Schaffer, and C. Xu, "Deep tissue multiphoton microscopy using longer wavelength excitation," Opt. Express **17**(16), 13354–13364 (2009).
15. M. E. Brezinski and J. G. Fujimoto, "Optical coherence tomography: High-resolution imaging in nontransparent tissue," IEEE J. Sel. Top. Quantum Electron. **5**(4), 1185–1192 (1999).
16. R. Aviles-Espinosa, S. I. C. O. Santos, A. Brodschelm, W. G. Kaenders, C. Alonso-Ortega, D. Artigas, and P. Loza-Alvarez, "Third-harmonic generation for the study of *Caenorhabditis elegans* embryogenesis," J. Biomed. Opt. **15**(4), 046020 (2010).
17. U. Keller, K. J. Weingarten, F. X. Kaertner, D. Kopf, B. Braun, I. D. Jung, R. Fluck, C. Hoenninger, N. Matuschek, and J. Aus der Au, "Semiconductor saturable absorber mirrors (SESAMs) for femtosecond to nanosecond pulse generation in solid-state lasers," IEEE J. Sel. Top. Quantum Electron. **2**(3), 435–453 (1996).
18. R. Aviles-Espinosa, G. Filippidis, C. Hamilton, G. Malcolm, K. J. Weingarten, T. Südmeyer, Y. Barbarin, U. Keller, S. I. C. O. Santos, D. Artigas, and P. Loza-Alvarez, "Compact ultrafast semiconductor disk laser: targeting GFP based nonlinear applications in living organisms," Biomed. Opt. Express **2**(4), 739–747 (2011).
19. Y. Zaouter, J. Didierjean, F. Balembois, G. Lucas Leclin, F. Druon, P. Georges, J. Petit, P. Goldner, and B. Viana, "47-fs diode-pumped Yb3+:CaGdAlO4 laser," Opt. Lett. **31**(1), 119–121 (2006).
20. C. R. Phillips, A. S. Mayer, A. Klenner, and U. Keller, "SESAM modelocked Yb:CaGdAlO4 laser in the soliton modelocking regime with positive intracavity dispersion," Opt. Express **22**(5), 6060–6077 (2014).

1. Introduction

Many applications such as multiphoton imaging [1], nanosurgery [2–5], and nanostructuring [6], require low-cost, compact, tunable, and high-peak-power ultrafast lasers. Compared to commercial Ti.Sapphire based lasers [7], commonly used for multiphoton imaging, Yb based lasers [8] enable direct diode pumping of high power ultrashort pulse lasers. The direct diode pumping drastically lowers the complexity of the laser, resulting in higher reliability and a cost-effective laser.

However, the drawback of Yb based ultrafast oscillators for biomedical imaging is their limited emission bandwidth and therefore the laser tenability [9,10]. The limited tunability could be addressed by a proper choice of a subsequent nonlinear fiber system. Microstructured or photonic crystal fibers [11] are typically used for spectral broadening and supercontinuum generation [12]. Nowadays, the photonic crystal fibers are matured technology and they are commercially available as standard fiber patchcords with standard connectors and a jacket protection [13].

When compared to laser central wavelength at 800 nm, the central wavelength above 1 micron is beneficial for multiphoton imaging and cell surgery owing to less scattering for most biomedical tissues [14,15]. These wavelengths could be challenging or impossible to reach with Ti:Sapphire based laser systems. In addition, the excitation wavelength above 1 micron, compared to 800 nm excitation wavelength, facilitates the detection due to higher camera sensitivities for the SHG and THG imaging modalities [16].

The Yb oscillator features low noise, robust self-starting, and long-term stability owing to SESAM modelocking [17] mechanism, already well-established in the ultrafast laser community. The low noise and long-term stability oscillator characteristics are critical for the low noise and long-term stability output from the highly nonlinear fiber, used for multiphoton imaging.

There are a number of laser parameters important to consider when optimizing the signal in multiphoton microscopy. Here we introduce the figure of merit (FOM) for the lasers used in multiphoton microscopy. The FOM narrows down the number of laser parameters important to estimate the highest microscopy signal and therefore facilitates the discussions, comparison and estimates about the various lasers for non-linear microscopy.

Finally, we demonstrate the developed laser system potential for nonlinear microscopy [18] by obtaining high-signal-to-noise ratio (SNR) two-photon excitation fluorescence (TPEF) images of a mouse intestine section labeled with different dyes. This laser system enables both multimodal microscopy and nanosurgery and should have advantages in wavelength and peak power over the typically used laser systems [5].

#212997 - $15.00 USD Received 28 May 2014; revised 18 Jun 2014; accepted 19 Jun 2014; published 26 Jun 2014
(C) 2014 OSA

2. Laser system description

The tunable laser system layout is depicted in Fig. 1. The high-power, low-noise, SESAM-modelocked, Yb-tungstate, solid-state laser generates 2.5 W of average power, 230 fs pulse duration, at 1040 nm central wavelength, with 80 MHz pulse repetition rate. The Yb oscillator output is coupled, after attenuating its average power down to 0.7W, into a highly non-linear fiber with coupling efficiency up to 90%. The oscillator spectrum is broadened into relatively smooth spectrum covering 800 to 1250 nm central wavelength range. Subsequently, the broadened spectrum is sliced and compressed by a standard prism compressor down to 25 fs pulse duration. The average power of each selected spectral slice is up to 150 mW, for a slice bandwidth of approximately 100 nm.

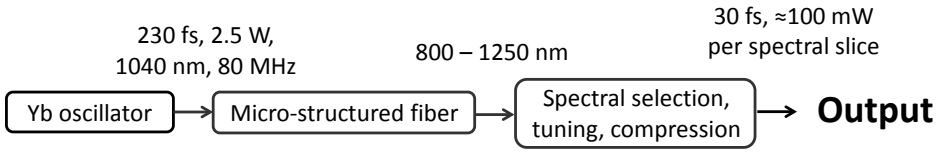

Fig. 1. The tunable laser system layout.

Figure 2 depicts a typical total laser system output. The black curve in Fig. 2(a) represents the whole broadened spectral output, while the red curve shows one selected spectral slice with FWHM of approximately 100 nm, centered at 960 nm. The spectral selection and tuning is performed with a slit in the prism compressor. The slit width, defining the spectral width is optimized for the shortest pulse without excessive side pulses or wings.

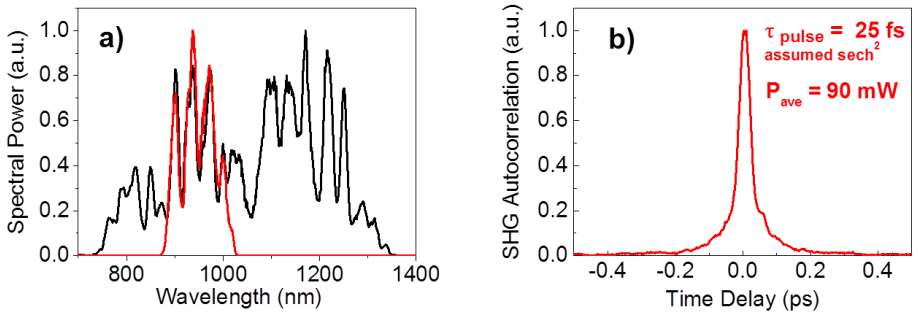

Fig. 2. (a) The total spectrally broadened laser system output (black curve) and selected spectrum with FWHM of approximately 100 nm, centered at 960 nm (red curve). (b) Aurocorrelation of the pulse, compressed down to 25 fs pulse duration.

In Fig. 2(b) we demonstrate the compressibility of a selected spectral slice. The spectral slice shown in Fig. 2(a) (red curve) is compressed to pulse duration of 25 fs. Figure 2(b) depicts the second harmonic generation intensity autocorrelation trace corresponding to pulse duration of 25 fs, assuming $sech^2$ pulse shape. Low level pulse wings are present in the autocorrelation trace owing to the third order dispersion that is not perfectly compensated.

The tunability and compression of the selected spectral slices are shown in Fig. 3. For the majority of the broadened spectral range, the pulses preserve a high degree of coherence and are compressed to approximately 30 fs pulse duration. The maximum average power is obtained at $\lambda = 1150$ nm, consistent with a region of high spectral density in the broadened spectrum in Fig. 2(a). The tunability of the laser system is limited by the width of the broadened spectrum after the microsctructured fiber.

#212997 - $15.00 USD Received 28 May 2014; revised 18 Jun 2014; accepted 19 Jun 2014; published 26 Jun 2014
(C) 2014 OSA

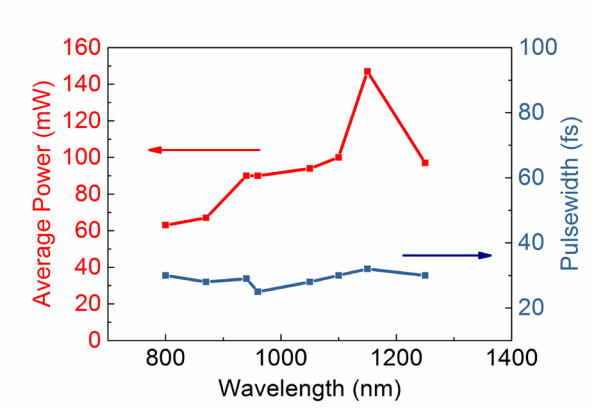

Fig. 3. Compressed laser system output pulse average power and duration versus central wavelength for a 100 nm selected spectral slice.

3. Figure of merit (FOM)

To optimize the laser parameters for multiphoton imaging, we propose a figure of merit (FOM) for the detected signal in the two-photon fluorescence microscope (TPF signal), which is proportional to the average power of the second harmonic signal. The main laser parameters are: average power $P_{average}$, pulse duration τ, pulse repetition rate R and the central wavelength λ. One can calculate the pulse peak power P_{peak} as follows:

$$P_{peak} = \frac{P_{average}}{R\tau} \tag{1}$$

The peak power of the second harmonic signal (or two-photon fluorescence signal) is:

$$P_{peak}(2\omega) = kP_{peak}{}^{2}(\omega) \tag{2}$$

where k is a constant factor. If one plugs Eq. (2) into Eq. (1) and solves it for average power of the second harmonic, the repetition rate and the pulse duration cancel out in the FOM expression, narrowing down from 4 related laser parameters to 2:

$$FOM \approx P_{average}(2\omega) \approx P_{average}(\omega) P_{peak}(\omega) \tag{3}$$

Thus, one can increase the TPF microscopy signal by increasing the peak or average power of the IR (fundamental) laser beam. A FOM with 2 instead of 4 (related) laser parameters helps in optimization of the laser design for a particular multiphoton application. Furthermore, one can generalize the FOM for the n-photon nonlinear process:

$$FOM_n \approx P_{average}(n\omega) \approx P_{average}(\omega) P_{peak}{}^{n-1}(\omega) \tag{4}$$

In our system, the peak power of the complete laser system output is limited by the fiber damage. While keeping the laser output peak power constant, we can increase the oscillator repetition rate twice and increase the oscillator average power twice. Therefore, compared to 40 MHz, the 80 MHz system increases twice the figure of merit (FOM) for TPF imaging.

In Fig. 4 we map the FOM of our 40 MHz system used for imaging (50 mW, 30 fs), the optically pumped VECSEL [18] (287 mW, 1.5 ps, 500 MHz), our 80 MHz Yb oscillator output prior to the fiber (2.5 W, 230 fs), and a typical Ti:Sapphire oscillator (2 W, 100 fs, 80 MHz). Our imaging system exhibits FOM of 2100 W^2, almost 20 times higher than the OP VECSEL with FOM of 110 W^2, sufficient for TPE imaging [18]. Yb and Ti:Sapphire oscillators with FOM of 340 000 W^2 and 500 000 W^2 must be strongly attenuated to prevent tissue damaging.

#212997 - $15.00 USD Received 28 May 2014; revised 18 Jun 2014; accepted 19 Jun 2014; published 26 Jun 2014
(C) 2014 OSA

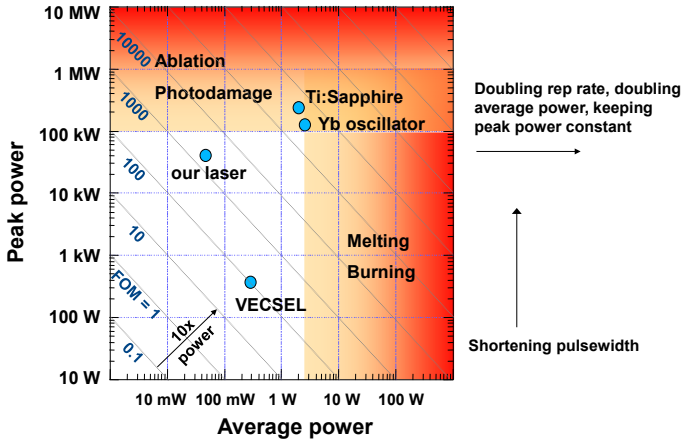

Fig. 4. Figure of merit (FOM) map of our imaging laser system, optically pumped VECSEL [18], our Yb oscillator, and a typical Ti:Sapphire laser. Regions in red correspond to FOMs not suitable for imaging due to different power-related effects.

4. Two-photon fluorescence (TPF) imaging

We used an Yb oscillator laser unit with 40 MHz pulse repetition rate for TPF imaging. The rest of the system was the same, as depicted in Fig. 1, but the final output average power was only up to 70 mW. With the 80 MHz repetition rate lasers system the FOM would be twice higher. Therefore, the images are expected to be brighter or faster imaging would be feasible. However, even with the 40 MHz laser we obtained excellent images and demonstrated the laser potential for multiphoton, multimodal imaging.

A spectral slice centered at 960 nm, with 50 mW of average laser output power, was used to obtain TPF images of a mouse intestine section, as shown in Fig. 5. Mouse intestine was labeled with Alexa Fluor 350 WGA (mucus of goblet cells), Alexa Fluor 568 phalloidin (filamentous actin prevalent in the brush border), and SYTOX Green nucleic acid stain (nuclei of goblet cells). The average power at the microscope sample plane was 5 mW.

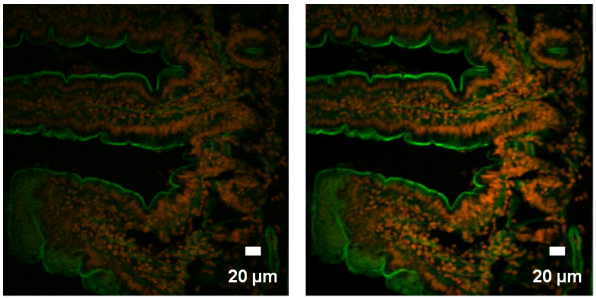

Fig. 5. Spectrally resolved image of mouse intestine section without averaging (left), and with 10 frames averaging (right). Alexa Fluor is depicted green and SYTOX Green red.

The images are acquired without (Fig. 5 left) and with 10 frames averaging (Fig. 5 right). At the used wavelength it was possible to excite Alexa Fluor 568 (one photon absorption peak at 579 nm) and SYTOX green (one photon absorption peak at 504 nm), while the excitation wavelength was out of range of the absorption peak for Alexa Fluor 350, at 343 nm. Even though the wavelength was not optimized for the dyes absorption peaks, the resulting images feature a high signal-to-noise ratio (SNR), due to the system compressor ability to adjust for the highest peak power (shortest pulse) at the sample plane of the microscope. The ability to obtain such a high SNR images without averaging demonstrates the laser system potential.

#212997 - $15.00 USD Received 28 May 2014; revised 18 Jun 2014; accepted 19 Jun 2014; published 26 Jun 2014
(C) 2014 OSA

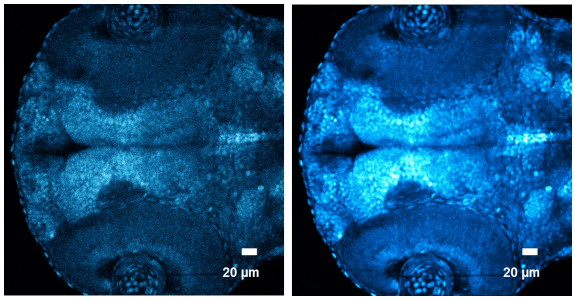

Fig. 6. Fixed zebra fish embryo imaging with the residual oscillator beam. Single frame image, without averaging is shown on the left, and with 10 frames averaging on the right.

The residual part of the oscillator beam, which is not coupled into the microstructured fiber is used for imaging at 1040 nm. Spectrally resolved image of zebra fish embryo is shown in Fig. 6 with single frame image, without averaging on the left, and with 10 frames averaging on the right. In this case the power at the sample plane was 50 mW. The zebra fish embryo was labeled using Td:tomato, with an absorption peak at 554 nm. Therefore, the oscillator wavelength was ideally suited for imaging purposes, resulting in high quality images.

5. Summary

We have developed a relatively simple and potentially low-cost laser system consisting of a high power, low-noise, SESAM modelocked Yb-doped solid-state laser, coupled into a micro-structured fiber, followed by a simple prism compressor performing also the spectral selection. Compressibility of the output laser pulses to 30 fs within the tunable range of 800 to 1250 nm, demonstrates the high degree of coherence in the generated continuum.

We introduced a figure of merit (FOM) for the lasers used for nonlinear microscopy, which is a product of peak and average power of the fundamental beam, for the two-photon processes.

Using this novel laser system, we have performed high signal-to-noise ratio TPF imaging of a mouse intestine section with 30 fs pulse duration, 5 mW average power at the sample plane, at 960 nm. Zebra fish embrio is imaged with 50 mW at the sample plane, at 1040 nm.

In the future, we will develop Yb:CALGO [19,20] material oscillator instead of Yb tungstate, and achieve shorter sub-100 fs pulses from the oscillator with higher repetition rate. Shorter pulses will generate broader spectrum and increase the tunability range. The higher pulse repetition rate will increase the FOM of the laser resulting in increased multi photon microscopy signal. From the microscopy aspect, the system is especially suitable for nonlinear imaging followed by the cell surgery of the identified targets. Here, imaging can be performed by the tunable 30 fs pulses, while the residual oscillator beam at 1040 nm with average power of 1 W can be used for cell surgery, which requires higher peak power.

Acknowledgments

This work was partially supported by the EU FP7 program: Marie Curie International Incoming Fellowship “UltraTune” (grant agreement number 251276), IP Collaborative project “FastDot” (grant agreement number 224338), and the NEXPRESSO program. In addition, this research has received funding from LASERLAB-EUROPE (FP7 grant agreement n° 284464) and also has been partially supported by Fundació Cellex Barcelona and partially conducted at ICFO’s Super-Resolution Light Nanoscopy Facility.

#212997 - $15.00 USD Received 28 May 2014; revised 18 Jun 2014; accepted 19 Jun 2014; published 26 Jun 2014
(C) 2014 OSA